

# Electron acceleration at the solar flare reconnection outflow shock

G. Mann<sup>1</sup>, H. Aurass<sup>1</sup>, and A. Warmuth<sup>1</sup>

Astrophysical Institute Potsdam (AIP), An der Sternwarte 16, 14482 Potsdam, Germany

Received February 10, 2005; accepted ?

**Abstract.** During solar flares a large amount of nonthermal electromagnetic radiation up to the  $\gamma$ -ray range is emitted from the corona implying the generation of energetic electrons. Within the framework of the magnetic reconnection scenario, jets appear in the outflow region and can establish standing fast-mode shocks if they penetrate with a super-Alfvénic speed into the surrounding plasma. These shocks can be a source of energetic electrons. During the solar event on October 28, 2003 an enhanced flux of hard X- and  $\gamma$ -rays up to an energy of 10 MeV has been observed by the INTEGRAL spacecraft indicating the generation of relativistic electrons. The radio signature of a standing shock wave appeared simultaneously with the enhanced hard X- and  $\gamma$ -ray fluxes. Here, this shock is assumed to be the source of the highly energetic electrons needed for the hard X- and  $\gamma$ -ray as well as the nonthermal radio radiation. The electrons are energized by shock drift acceleration, which is necessarily treated in a fully relativistic manner. After acceleration, the electrons travel along the magnetic field lines towards the denser chromosphere, where they emit hard X- and  $\gamma$ -ray radiation via bremsstrahlung. With the obtained theoretical results, the observed photon fluxes in the range 7.5–10 MeV are explained by the theoretically obtained results adopting the coronal conditions found for the event on October 28, 2003.

**Key words.** acceleration of particles — shock waves — Sun: flares — Sun: X-rays — Sun: radio radiation

## 1. Introduction

In October/November 2003 several flares of X-class importance were observed. Especially, the event on October 28, 2003 showed a strong enhancement of the hard X- and  $\gamma$ -ray radiation as observed by the INTEGRAL (Gros et al. 2004) and RHESSI (Lin et al. 2002) spacecraft. Hard X- and  $\gamma$ -ray radiation is generated by relativistic electrons, which are initially accelerated by the flare process in the corona and, subsequently, travel along the magnetic field lines towards the denser chromosphere, where they emit electromagnetic radiation via *bremsstrahlung* (see e. g. Brown (1971, 1972)). Thus, the appearance of hard X- and  $\gamma$ -ray radiation implies the generation of highly energetic electrons during the flare process.

If a prominence (EP) is destabilized and, subsequently, rises up, stretching the underlying magnetic field lines (Fig. 1). That leads to the formation of a current sheet. If the current is exceeding a critical value there, the resistivity is suddenly increased by plasma waves excitation due to various instabilities (see e. g. Treumann and Baumjohann (1997)). Then, magnetic reconnection can take place in the region of enhanced resistivity (also called *diffusion region* (DR)). Due to the strong curvature of the magnetic field lines in the vicinity of the diffusion region

the slowly inflowing plasma is shooting away from the reconnection site as a hot jet (see Fig. 1). If the speed of these jets is super-Alfvénic, a fast magnetosonic shock, also called *termination shock* (TS) can be established due to the deceleration of the jet. The appearance of such shocks is predicted in the numerical simulations by Forbes (1986) and Shibata et al. (1995).

As well-known, only electric fields are able to accelerate electrons. An electric field is induced within the diffusion region, where electrons can directly be accelerated (Holman 1985, Benz 1987, Litvinenko, 2000). Since the real phase space of the diffusion region is very small, Tsuneta and Naito (1998) proposed that the shock wave established in the outflow region of the reconnection site could be the source of the energetic electrons needed for the hard X-ray radiation during flares. Aurass et al. (2002) and Aurass & Mann (2004) firstly reported on radio signatures of such shocks.

The solar event on October 28, 2003 has revealed that the hard X- and  $\gamma$ -ray fluxes are associated with the radio spectral signature of the TS during the impulsive phase of the flare (Section 2). Therefore, this shock is considered as the source of the energetic electrons needed for the hard X- and  $\gamma$ -ray emission. The generation of highly relativistic electrons via *shock drift acceleration* is investigated

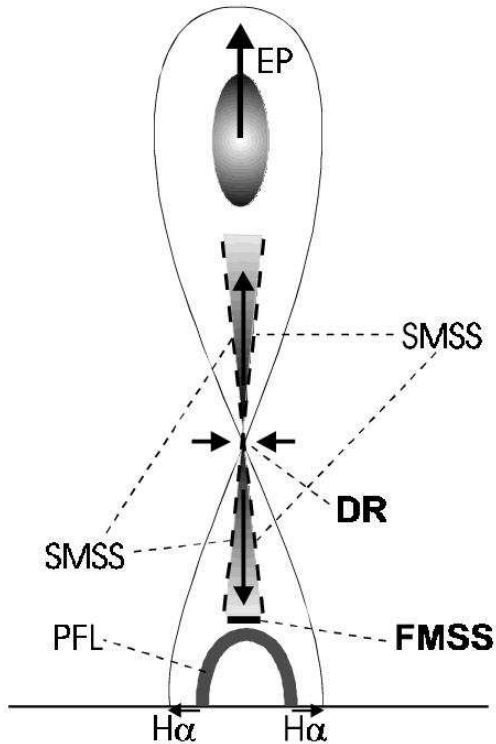


**Fig. 1.** Sketch of the generation of the termination shock (TS) at the flare (EP, erupting prominence; DR, diffusion region; SMSS, slow-mode standing shock; FMSS, fast-mode standing shock also called termination shock (TS); PFL, post-flare loop). The grey shaded areas with the black arrows show the reconnection outflow jets.

in Section 3. The theoretically obtained results are compared with the observations in Section 4.

## 2. Observations

On 28 October 2003 a huge X17 flare occurred in active regions NOAA 10486–10491 between 09:51 and 12:00 UT. The event became impulsive at 11:01 UT after a slow and intermittent rise of energy release. Gros et al. (2004), Share et al. (2004), Miroshnichenko et al. (2005), and Bieber et al. (2005) discussed hard X- and  $\gamma$ -ray as well as particle data of this most intense solar energetic particle event of cycle 23 (Gopalswamy et al. 2005).

During a short time interval between 11:02:30 and 11:04:30 UT of the impulsive flare phase, the dynamic radio spectrum recorded by the radio spectralpolarimeter (40–800 MHz) of the Astrophysical Institute Potsdam (Mann et al. 1992) showed two harmonically related roughly non-drifting lanes in the frequency range between 100 and 500 MHz. They can doubtlessly be identified as fundamental (F) and harmonic (H) type II burst-like emission, since they show the typical components of such bursts, i. e. here the (non-drifting) “backbone” and the “herringbones” (HB) shooting away from the backbone towards both higher and lower frequencies (see e. g.

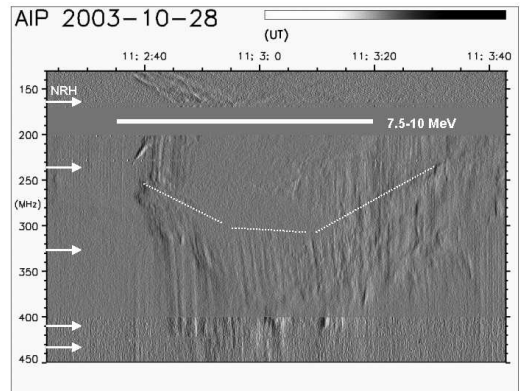


**Fig. 2.** The time-derived dynamic radio spectrum of the 28 October 2003 X-class flare shows type II burst emission associated with the flare TS (gap between 170 and 200 MHz due to local TV). Given is the frequency range of the Nançay radio heliograph (NRH, white arrows—the observing frequencies, compare the imaging data in Fig. 3) and the time interval of significant enhancement of 7.5–10 MeV (white bar, after Gros et al. 2004). Fast drift features leaving the slightly curved backbone toward higher and lower frequencies are herringbone (HB) fine structures. Between 130 and 170 MHz: high frequency edge of F-mode. Above 200 MHz: H-mode emission. The dashed white line roughly marks the onset of HB emission toward high frequencies. In the H-mode the backbone bandwidth is  $< 40$  MHz (upper limit of band splitting).

Nelson & Melrose (1985) and Mann (1995) for reviews). In two previous papers (Aurass et al. 2002, Aurass & Mann 2004)) it was shown that such spectral signatures can be interpreted as the radio signature of the TS which is formed in the lower and, possibly, also in the upper reconnection outflow jet during the flare (see Fig. 1).

Figure 2 shows the time derivative of the dynamic spectrum around the above mentioned time interval. The frequency range encloses the five imaging frequencies (white arrows in Fig. 2) of the Nançay radio heliograph (NRH, Kerdraon et al. 1996). The spectral feature with the fast drifting HBs is regarded as the radio signature of the lower TS. For the first time this feature is identified in both harmonic modes. This reveals that the shock-related radio source acts at the 150 MHz level in the corona.

The present case is exceptional because X- and  $\gamma$ -ray data (Gros et al. 2004) show a strong enhancement of photon fluxes up to the 10 MeV range just during the appearance of the TS radio spectral features (white bar in Fig. 2). This proves that the TS radio signature simultaneously occurs with a very efficient energization of a large amount of electrons.

In Figure 3, a composed map of radio imaging information is presented for 11:03:12 UT, i. e. in the time interval of the TS occurrence. The map is overplotted on a SOHO-MDI image (Scherrer et al. 1995) with isolines of the photospheric longitudinal magnetic field. The hard X-ray sources seen by RHESSI (Lin et al. 2002) are additionally shown as “+”. Unfortunately RHESSI only observed after 10:06 UT.

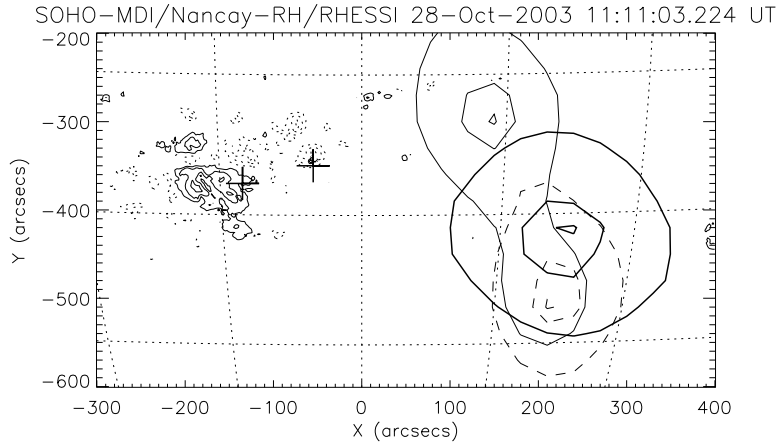


**Fig. 3.** Radio sources during termination shock emission, 11:03:12 UT (compare Fig. 2). For simplicity, we show here only three of five NRH imaging frequencies being harmonic mode TS emission; for NRH 432 MHz (thin continuous), 410.5 (dashed), and 327 MHz (thick continuous). Small-scale isolines: SOHO MDI 11:11:30 UT longitudinal field magnetogram, lines at .5, 1, 1.5 and  $2 \cdot 10^3$  Gauss revealing the dominant field structures of NOAA AR 10486. Large crosses (+) over the active region give the RHESSI hard X-ray source centroids 11:06–11:10 UT. The TS radio source is situated at least  $0.3 R_{\odot}$  away of AR 10486. 150 arcsecs are taken for a characteristic equivalent half-power source diameter leading to an area of  $A_{source} = 2.9 \cdot 10^{20} \text{ cm}^2$  as used in Section 4.

Just before the appearance of the TS in the dynamic radio spectrum, a radio source is situated above the active region NOAA 10486. After the onset of the TS (see Fig. 3), the corresponding radio source occurs far away from the flare ribbons. If seen over time, the source is firstly formed at 432–327 MHz, changes from simple to double-split at the highest frequencies of the H-mode, and also in the F-mode. The TS source occurs in projection about  $0.3 R_{\odot} = 210 \text{ Mm}$  away from chromospheric flare signatures and outside of the flaring active region but in the direction of one branch of the later visible CME. Note that the double source structure visible at 432 MHz in Fig. 3 fits well with rising but inclined and somewhat twisted post-flare loops above NOAA 10486 having footpoints near the RHESSI sources (“+” in Fig. 3, remind also Fig. 1).

Now, the TS is considered to be not only the source of the related type II burst-like radio waves but also of the energetic electrons which are generated by shock drift acceleration.

### 3. Relativistic shock drift acceleration

Fast magnetosonic shocks are accompanied with a density and magnetic field compression (see e. g. Priest (1982)). Consequently, they represent moving magnetic mirrors at which charged particles can be accelerated. Here, the TS is considered to be the source of energetic electrons which are generated via shock drift acceleration. Since it is intended to explain the production of highly energetic electrons ( $\approx 10 \text{ MeV}$ ) as observed during the solar event on October 28, 2003, the shock drift acceleration must necessarily be treated in a fully relativistic manner (see e. g. Ball & Melrose (2001) for the non-relativistic approach).

The shock wave is put in the z-y plane and moves with the speed  $v_s$  along the x axis. The upstream mag-

netic field  $\mathbf{B}_{up}$  is located in the z-x plane and takes an angle  $\theta$  towards the x axis, i. e.  $\mathbf{B}_{up} = B_{up}(\cos \theta, 0, \sin \theta)$ . Generally, shock drift acceleration represents a transformation of the particle velocities parallel and perpendicular to the magnetic field, i. e.  $\{V_{i,\parallel}; V_{i,\perp}\} \rightarrow \{V_{r,\parallel}; V_{r,\perp}\}$ . Here, the indices “i” and “r” denote the state before and after the reflection, respectively. The reflection process is usually performed in the de Hoffmann-Teller frame, where the shock is at rest and the motional electric field is removed, i. e. the upstream plasma flow is directed along the upstream magnetic field in this frame. Then,  $v_s \sec \theta$  is the shock speed in the de Hoffmann-Teller frame. According to the addition theorem of relativistic velocities (Landau and Lifschitz 1982), the particle velocities in the de Hoffmann-Teller frame are related to the initial ones by

$$\beta_{i,HT,\parallel} = \frac{\beta_{i,\parallel} - \beta_s}{1 - \beta_{i,\parallel}\beta_s} \quad (1)$$

and

$$\beta_{i,HT,\perp} = \frac{\beta_{i,\perp}}{1 - \beta_{i,\parallel}\beta_s} \cdot \sqrt{1 - \beta_s^2} \quad (2)$$

with  $\beta_{i,\parallel} = V_{i,\parallel}/c$ ,  $\beta_{i,\perp} = V_{i,\perp}/c$ , and  $\beta_s = v_s \sec \theta/c$ . The reflection takes place under the conservation of the kinetic energy

$$\beta_{HT,\parallel}^2 + \beta_{HT,\perp}^2 = const \quad (3)$$

and the magnetic moment

$$\frac{\beta_{HT,\perp}^2}{B} = const \quad (4)$$

resulting into  $\beta_{r,HT,\parallel} = -\beta_{i,HT,\parallel}$  and  $\beta_{r,HT,\perp} = \beta_{i,HT,\perp}$ .  $B$  denotes the magnitude of the magnetic field. The influence of the electrostatic potential across the shock can be

neglected when relativistic particles are considered, since it is of order of a few  $k_B T$  ( $k_B$ , Boltzmann's constant;  $T$ , temperature in the upstream region). It is given by

$$e\phi_{HT} = \frac{\gamma}{(\gamma-1)} \cdot k_B T \cdot \left[ \left( \frac{N_{down}}{N_{up}} \right)^{(\gamma-1)} - 1 \right] \quad (5)$$

( $\gamma$ , ratio of the specific heats) in the de Hoffmann-Teller frame (Goodrich and Scudder 1984, Kunic et al. 1999).  $N_{down}$  and  $N_{up}$  denote the particle number densities in the down- and upstream region, respectively. Because of  $N_{down}/N_{up} \leq 4$  for fast magnetosonic shocks (see e. g. Priest (1982)) Eq. (5) provides  $e\phi_{HT} \leq 3.8k_B T$  for  $\gamma = 5/3$ .

After performing the reflection process with fulfilling of the conservation laws (see Eqs. (3) and (4)) the particle velocities are transformed from the de Hoffmann-Teller frame back to the laboratory frame by

$$\beta_{r,\parallel} = \frac{\beta_{r,HT,\parallel} + \beta_s}{1 + \beta_{i,HT,\parallel}\beta_s} \quad (6)$$

and

$$\beta_{r,\perp} = \frac{\beta_{r,HT,\perp}}{1 + \beta_{i,HT,\parallel}\beta_s} \cdot \sqrt{1 - \beta_s^2} \quad (7)$$

Finally, the particles velocities after the reflection are related to those in the initial state by

$$\beta_{r,\parallel} = \frac{2\beta_s - \beta_{i,\parallel}(1 + \beta_s^2)}{1 - 2\beta_{i,\parallel}\beta_s + \beta_s^2} \quad (8)$$

and

$$\beta_{r,\perp} = \frac{(1 - \beta_s^2)}{1 - 2\beta_{i,\parallel}\beta_s + \beta_s^2} \cdot \beta_{i,\perp} \quad (9)$$

where the Eqs. (1) and (2) are inserted into Eqs. (6) and (7). In the non-relativistic limit Eqs. (8) and (9) transfer into the well-known ones, i. e.  $V_{r,\parallel} = 2v_s \sec \theta - V_{i,\parallel}$  and  $V_{r,\perp} = V_{i,\perp}$  (Holman and Pesses 1982, Ball and Melrose 2003).

Additionally, the reflection conditions

$$\beta_{i,\parallel} \leq \beta_s \quad (10)$$

and

$$\beta_{i,\perp} \geq \frac{\tan \alpha_{lc}}{\sqrt{1 - \beta_s^2}} \cdot (\beta_s - \beta_{i,\parallel}) \quad (11)$$

must be satisfied by the initial particles in order to be accelerated. The loss-cone angle is defined by  $\alpha_{lc} = \arcsin[(B_{up}/B_{down})^{1/2}]$ , where  $B_{down}$  denotes the magnitude of the magnetic field in the down-stream region.

Thus, the acceleration process basically represents a transformation in the  $\beta_{\perp} - \beta_{\parallel}$  plane as illustrated in Figure 4. For a shock wave with  $\beta_s = 0.8$  and  $B_{down}/B_{up} = 2$ , i. e.  $\alpha_{lc} = 45^\circ$ , the initial particles located in the grey area left from the dashed line are transformed into the dark one to the right from it.

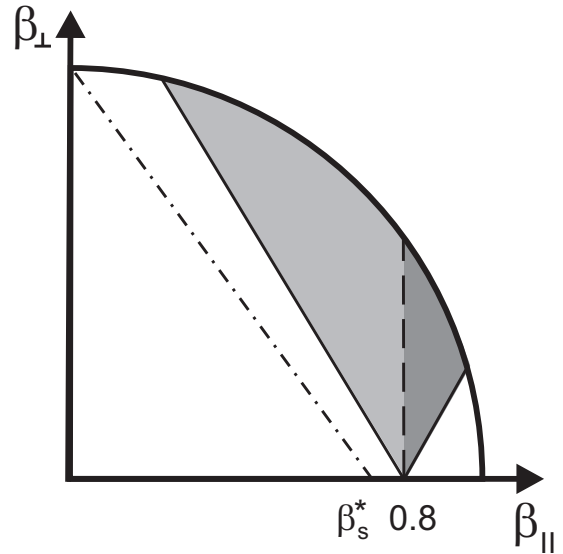


**Fig. 4.** Illustration of the shock drift acceleration in the  $\beta_{\perp} - \beta_{\parallel}$  plane. For a shock wave with  $\beta_s = 0.8$  and  $B_{down}/B_{up} = 2$ , all particles in the grey area are transformed into the dark area. In the same case all particles located right from the dashed-dotted line will be transmitted into the downstream region at a second encounter (see further explanation in Sec. 3 and 4.)

It should be emphasized that there is a critical shock speed  $\beta_s^*$ . Only particles with an initial velocity  $\beta_{i,\parallel} > 0$  will be accelerated by shock waves with  $\beta_s > \beta_s^* = \cos \alpha_{lc}$  (see also Fig. 4). The other particles moving towards the shock in the laboratory frame, i. e.  $\beta_{i,\parallel} < 0$ , will totally be transmitted into the downstream region.

## 4. Discussion

The radio images of TS are observed around 300 MHz. It is the H-mode emission as revealed from the spectral radio data (Fig. 2). Therefore, the plasma parameters usually found at the 150 MHz level in the corona will be chosen as the basic parameters for the presented discussion. An electron number density of  $N_0 = 2.8 \cdot 10^8 \text{ cm}^{-3}$  is related to this frequency. According to a twofold Newkirk (1961) coronal density model the 150 MHz level is located about 160 Mm above the photosphere. There, a magnetic field strength of 4.7 G can be expected above active regions (Dulk and McLean 1978). Furthermore, a typical flare temperature of  $10^7 \text{ K}$  is assumed for the discussion. All these parameters result in a thermal electron velocity  $v_{th,e} = 12300 \text{ km/s}$  and an Alfvén speed  $v_A = 610 \text{ km/s}$ .

For the TS a jump of the density  $N_{down}/N_{up} = 2$  (Aurass et al. 2002) is assumed because of the bandwidth of the non-drifting type II burst (Fig. 3). According to the Rankine-Hugoniot relationships (see e. g. Priest (1982)) it leads to a magnetic field compression  $B_{down}/B_{up} = 2$  across the shock and an Alfvén-Mach number  $M_A = 2.3$ , i. e. the shock speed is  $v_s = 1500 \text{ km/s}$ . From the radio images an area  $A_{source} = 2.9 \cdot 10^{20} \text{ cm}^2$  is derived for the TS-associated radio source (Fig. 3). Consequently,

the total electron flux through the shock is found to be  $P_e = N_0 \cdot A_{source} \cdot v_A \cdot M_A = 1.1 \cdot 10^{37} \text{ s}^{-1}$ .

In order to determine the phase space density for the accelerated electrons, a velocity distribution function of electrons in the upstream region has to be introduced. In-situ spacecraft measurements (Lin 1974) showed that electron distribution functions are usually not Maxwellian ones but have an enhanced supra-thermal tail in space plasmas. Thus, a *kappa distribution* defined by

$$f = C_\kappa \cdot \left[ 1 + \frac{E}{\kappa E_\kappa} \right]^{-\kappa-1} \quad (12)$$

with the kinetic energy  $E = m_0 c^2 [(1 - \beta^2)^{-1/2} - 1]$  (see e. g. Maksimovich et al, (1997) and Pierrard et al. (1999)) is used for the initial velocity distribution for electrons in the upstream region for further discussions. Note that for energies  $E \approx E_\kappa$  and  $E \gg E_\kappa$  the kappa distribution behaves like a Maxwellian and a power-law one, respectively. In the limit  $\kappa \rightarrow \infty$  it totally transfers into a Maxwellian distribution. Here, the distribution function is normalized to unity by fixing the constant  $C_\kappa$ , i. e.

$$C_\kappa^{-1} = 4\pi c^3 \int_0^\infty d\epsilon \cdot \frac{\sqrt{\epsilon(2+\epsilon)}}{(1+\epsilon)^4} \cdot \left[ 1 + \frac{\epsilon}{\kappa \epsilon_\kappa} \right]^{-\kappa-1} \quad (13)$$

with  $\epsilon = E/m_0 c^2$  and  $\epsilon_\kappa = E_\kappa/m_0 c^2$ . According to the kinetic definition of the temperature  $\bar{E} = 3N_0 k_B T/2$  or

$$\bar{\epsilon} = \frac{\bar{E}}{m_0 c^2} = \frac{3}{2} \cdot \frac{k_B T}{m_0 c^2} = 4\pi C_\kappa c^3 \cdot \int_0^\infty d\epsilon \cdot \epsilon \cdot \frac{\sqrt{\epsilon(2+\epsilon)}}{(1+\epsilon)^4} \left[ 1 + \frac{\epsilon}{\kappa \epsilon_\kappa} \right]^{-\kappa-1} \quad (14)$$

the parameter  $\epsilon_\kappa$  is related to the temperature T by

$$\epsilon_\kappa = \frac{(\kappa - 3/2)}{\kappa} \cdot \frac{k_B T}{m_0 c^2} \quad (15)$$

After introducing the pitch angle  $\vartheta$  according to  $\beta_{\parallel} = \beta \cdot \cos \vartheta$  the number of electrons  $dN$  in the range  $[\epsilon + d\epsilon, \epsilon]$  and  $[\vartheta + d\vartheta, \vartheta]$  can be given by

$$\frac{1}{N_0} \cdot \frac{dN}{d\vartheta d\epsilon} = 2\pi C_\kappa c^3 \sin \vartheta \cdot \frac{\sqrt{\epsilon(2+\epsilon)}}{(1+\epsilon)^4} \cdot \left[ 1 + \frac{\epsilon}{\kappa \epsilon_\kappa} \right]^{-\kappa-1} \quad (16)$$

The Figure 5 shows the energy dependence of  $N_0^{-1} \cdot dN/d\epsilon$  for a temperature of  $10^7$  K and  $\kappa = 2.5, 10,$  and  $\infty$  after integrating with respect to the pitch angle  $\vartheta$ . As already mentioned the case with  $\kappa = \infty$  corresponds to a Maxwellian distribution. A value  $\kappa = 10$  seems to be appropriate in the solar corona (Maksimovich et al. 1997, Pierrard et al. 1999).

In order to illustrate the generation of relativistic electrons by the proposed mechanism the production of 8.54 MeV ( $\epsilon = 16.68$ ) electrons is demonstrated as an example. Note that electrons of such an energy are needed for the emission of hard X- and  $\gamma$ -ray radiation up to 10 MeV, as observed by the INTEGRAL spacecraft during the event on October 28, 2003. An electron with an initial energy of 2.57 MeV ( $\epsilon = 5.03$ ) and an initial pitch

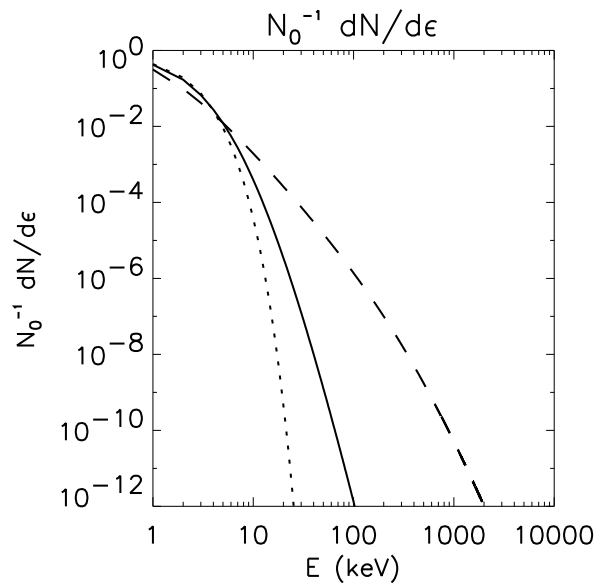


**Fig. 5.** The dependence of the function  $N_0^{-1} \cdot dN/d\epsilon$  on the energy E given in keV for a kappa-distribution with  $\kappa = 2.5$  (dashed line), 10 (full line), and  $\infty$  (dotted line). Note that  $\kappa = \infty$  corresponds to a Maxwellian distribution.

angle of  $6.74^\circ$  (i. e.  $\beta_{i,\parallel} = 0.9793$  and  $\beta_{i,\perp} = 0.1157$ ), is accelerated by a shock wave with a speed of 1500 km/s and an angle  $\theta = 89.7115^\circ$  ( $\beta_s = 0.993$ ) to a final state with an energy of 8.54 MeV and a pitch angle of  $2.25^\circ$  (i. e.  $\beta_{r,\parallel} = 0.9976$  and  $\beta_{r,\perp} = 0.0393$ ) via shock drift acceleration. Now, the number of 8.54 MeV electrons generated by this mechanism is determined. As previously demonstrated, such electrons are produced from electrons with an initial energy of 2.57 MeV and an initial pitch angle of  $6.74^\circ$ . The number of such electrons is  $N_0^{-1} \cdot dN/d\vartheta d\epsilon = 3.6 \cdot 10^{-28}$  (see Eq. (16)). For comparison, the number of electrons with an energy of 8.54 MeV and an pitch angle of  $2.25^\circ$  is found to be  $N_0^{-1} \cdot dN/d\vartheta d\epsilon = 2.4 \cdot 10^{-34}$  in the upstream region according to Eq. (16) if no acceleration would happen. Thus, the proposed acceleration mechanism enhances the number of 8.5 MeV electrons by a factor of  $1.5 \cdot 10^6$  in comparison to the state without any acceleration. Since the total flux of electrons through the shock is  $1.1 \cdot 10^{37} \text{ s}^{-1}$ ,  $4 \cdot 10^{11}$  electrons with an energy of 8.5 MeV are produced per second. That impressively demonstrates the efficiency of the proposed mechanism.

After the acceleration at the TS the electrons are reflected back towards the upstream region. Because of the curvature of the magnetic field lines in the outflow region of the reconnection site, the energized electrons will encounter the TS once more. Since the shock speed  $\beta_s = 0.993 > \beta_s^* = 0.707$  for  $\alpha_{IC} = 45^\circ$  because of  $B_{down}/B_{up} = 2$ , all electrons accelerated at the first shock encounter are totally transmitted into the downstream region at the second encounter. Then, they travel along the magnetic field lines towards the denser chromosphere, where they can emit hard X- and  $\gamma$ -ray radiation via bremsstrahlung.

## 5. Summary

During solar flares a large amount of electromagnetic radiation from the radio up to the hard X- and  $\gamma$ -ray range is emitted from the corona. Especially, the huge solar event on October 28, 2003 was accompanied with a strongly enhanced emission of hard X- and  $\gamma$ -ray radiation (up to  $\approx 10$  MeV) during the impulsive phase. Magnetic reconnection is one possible process for explaining a sudden energy release in the solar corona during flares. A jet of hot plasma is streaming away from the reconnection site. If the speed of this flow is super-Alfvénic, a shock wave (TS) can be established in the outflow region. The solar radio data showed signatures of such a shock just during the impulsive phase of this special event. The simultaneous appearance of enhanced photon fluxes up to 10 MeV and the radio signatures of the TS (see Sect. 2) imply that the TS is the source of those electrons which generate hard X- and  $\gamma$ -rays.

Here, the highly energetic electrons are considered to be generated by shock drift acceleration at the TS. That necessarily requires to generalize shock drift acceleration in a fully relativistic manner. Electrons with energies of about 10 MeV can only produced by a relativistic shock, which is connected with a nearly perpendicular shock geometry under coronal circumstances. With the adoption of the plasma parameters found in the corona during the event on October 28, 2003 it has been demonstrated that the proposed mechanism is able to provide the enhanced flux of 8.5 MeV electrons, required for the emission of hard X- and  $\gamma$ -ray radiation as observed by the INTEGRAL spacecraft. They are produced from electrons with an initial energy of about 2.5 MeV. If one had chosen a Maxwellian distribution with a temperature of  $10^7$  K for the electrons, significantly less than one 2.5 MeV electron would enter the shock area  $A_{source}$  per second. That demonstrates the necessity to choose a kappa distribution, which is anyway much more appropriate for space plasmas than a Maxwellian one (Lin et al. 1996, Vocks & Mann 2003).

The relativistic electrons produced at the TS can be the source of the nonthermal hard X- and  $\gamma$ -ray radiation in the chromospheric footpoints as well as at the loop-top areas. Additionally note that the proposed mechanism would also work for energetic protons (up to  $< 10$  GeV), since shock drift acceleration is basically independent from the charge of the particles.

We have shown that the generation of highly energetic electrons by the TS as is really able to explain the enhanced photon fluxes up to 10 MeV as observed by the INTEGRAL spacecraft during the solar event on October 28, 2003. The comprehensive observational and theoretical study confirms the idea of Tsuneta & Naito (1998) in a quantitative manner.

*Acknowledgements.* The authors thank G. Emslie, G. Holman, H. Hudson, R. P. Lin, and L. Vlahos for stimulating discussions during the 5th RHESSI Workshop in Locarno in June 2005. Further, we gratefully acknowledge the use of the SOHO-

MDI, RHESSI, and Nançay Multifrequency Radioheliograph data. The work was financially supported by the German space agency *Deutsches Zentrum für Luft- und Raumfahrt* (DLR) under grant No. 50 QL 0001.

## References

- Aurass, H. & Mann, G. 2004, *ApJ*, 615, 526  
 Aurass, H., Vršnak, B., & Mann, G. 2002, *A&A*, 384, 273  
 Ball, L. & Melrose, D. B. 2001, *Publ. Astron. Soc. Austr.* 18, 361  
 Benz, A. O. 1987, *Solar Phys.*, 111, 1  
 Bieber, J. W., Clem, J., Evenson, P., Pyle, R., Ruffolo, D. & Sáiz, A. 2005, *Geophys. Res. Lett.* 32, 302  
 Brown, J. C. 1971, *Solar Phys.*, 18, 489  
 Brown, J. C. 1972, *Solar Phys.*, 26, 441  
 Dulk, G. A. & McLean, D. J. 1978, *Solar Phys.*, 57, 235  
 Forbes, T. G. 1986, *ApJ* 305, 553  
 Goodrich, C. C. & Scudder, J. 1984, *J. Geophys. Res.*, 89, 6654  
 Gopalswamy, N., Barbieri, L., Lu, G. Plunkett, S. P., & Skoug, R. M. 2005, *Geophys., Res. Lett.* 32, 304  
 Gros, M., et al. 2004, *Proc. 5th INTEGRAL Workshop*,  
 Holman, G. D. 1985, *ApJ*, 293, 584  
 Holman, G. D. & Pesses, M. E. 1983, *ApJ*, 267, 837  
 Kunic, Z., Cairns, I. H., & Knock, S. A. 2002, *J. Geophys. Res.*, 107, 10,029  
 Landau, L. D. & Lifshitz, E. M. 1975, *The Classical Field Theory* (Pergamon Press, Tarrytown (N. Y.)), p. 264  
 Lin, R. P. 1974, *Sp. Sec. Rev.*, 16, 189  
 Lin, R. P., et al. 1996, *Geophys. Res. Lett.*, 94, 1211  
 Lin, R. P., et al. 2002, *Solar Phys.* 210, 3  
 Litvinenko, Y. E. 2000, in *High Energy Solar Physics - Anticipating HESSI*, ed. R. Ramaty & N. Mandzhavidze, ASPC Conference Ser. Vol. 206, p. 167  
 Maksimovic, M. Pierrard, V. & Lemaire, J. 1997, *A&A* 324, 725  
 Mann, G. 1995, in *Coronal magnetic Energy Release*, ed. A. O. Benz & A. Krüger (Lecture Notes in Physics, Springer Verlag, Heidelberg) pp. 183  
 Mann, G., Aurass, H., Voigt, W. & Paschke, J. 1992, in *Proc. 1st SOHO Workshop*, ESA-SP 348, 129  
 Miroshnichenko, L. I., et al. 2005, *Adv. Space Res.*, submitted  
 Nelson, G. S. & Melrose, D. 1985, *Type II Bursts*, in *Solar Radiophysics*, ed. D. J. McLean & N. R. Labrum (Cambridge University Press, Cambridge) pp. 333  
 Newkirk, G. A., 1961, *ApJ*, 133, 983  
 Pierrard, V., Maksimovic, M., & Lemaire, J. 1999, *J. Geophys. Res.* 104, 17,021  
 Priest, E. R. 1982, *Solar Magnetohydrodynamics* (Reidel Publ. Comp., Dordrecht)  
 Scherrer, P. H., Bogart, R. S., Bush, R. I. & 9 co-authors 1995, *Solar Phys.* 162, 129  
 hare04 Share, G., Murphy, R. J., Smith, D. M., & Schwartz, R. A. 2004, *ApJ* 615, L169  
 Shibata, K., Masuda, S., Shimojo, M., Hara, H., Yokoyama, T., Tsuneta, S., Kosugi, T. & Ogawara, Y. 1995, *ApJ* 451, L83  
 Treumann, R. A. & Baumjohann, W. 1997, *Advances Space Plasma Physics* (Imperial College Press, London) p. 143  
 Tsuneta, S. & Naito, T. 1998, *ApJ* 495, L67  
 Vocks, C. & Mann, G. 2003, *ApJ* 593, 1134